



Computation of spiking activity for a stochastic spatial neuron model: Effects of spatial distribution of input on bimodality and CV of the ISI distribution

Henry C. Tuckwell

Max Planck Institute for Mathematics in the Sciences, Inselstr. 22, Leipzig D-04103, Germany

Received 30 May 2006; accepted 18 August 2006

Available online 5 September 2006

Abstract

We obtain computational results for a new extended spatial neuron model in which the neuronal electrical depolarization from resting level satisfies a cable partial differential equation and the synaptic input current is also a function of space and time, obeying a first order linear partial differential equation driven by a two-parameter random process. The model is first described explicitly with the inclusion of all biophysical parameters. Simplified equations are obtained with dimensionless space and time variables. A standard parameter set is described, based mainly on values appropriate for cortical pyramidal cells. When the noise is small and the mean voltage crosses threshold, a formula is derived for the expected time to spike. A simulation algorithm, involving one-dimensional random processes is given and used to obtain moments and distributions of the interspike interval (ISI). The parameters used are those for a near balanced state and there is great sensitivity of the firing rate around the balance point. This sensitivity may be related to genetically induced pathological brain properties (Rett's syndrome). The simulation procedure is employed to find the ISI distribution for some simple patterns of synaptic input with various relative strengths for excitation and inhibition. With excitation only, the ISI distribution is unimodal of exponential type and with a large coefficient of variation. As inhibition near the soma grows, two striking effects emerge. The ISI distribution shifts first to bimodal and then to unimodal with an approximately Gaussian shape with a concentration at large intervals. At the same time the coefficient of variation of the ISI drops dramatically to less than 1/5 of its value without inhibition.

© 2006 Elsevier Inc. All rights reserved.

E-mail address: tuckwell@mis.mpg.de

0025-5564/\$ - see front matter © 2006 Elsevier Inc. All rights reserved.

doi:10.1016/j.mbs.2006.08.021

Keywords: Neuronal model; Stochastic model; Balanced inputs; Stochastic partial differential equation; Bimodal ISI distributions

1. Introduction

Stochastic aspects of neuronal activity have been energetically studied, especially after it had been pointed out they were important effects that needed explanation and elucidation [1,2]. Although it had been long realized that the spike trains of neurons in various structures in the mammalian central nervous system are highly variable [3–5], the meaning and significance of the random nature of such neuronal patterns of activity are still unclear. Stochastic models of neurons thus continue to be of much interest as exemplified by several recent articles with diverse approaches and diverse objectives of analysis [6–10]. Recently, the different ways in which, for example, cortical pyramidal cells, fire regular (not necessarily periodic) sets of spikes with current injection, but in apparently random fashion in vivo have been contrasted [11]. The issue was raised as to whether the stochasticity is in fact an integral part of the information transmission process. Indeed apparently random spontaneous activity has been found to play an important role in visual perception [12].

In a recent paper [13], a new stochastic spatial model neuron was introduced in which the voltage satisfied the usual linear cable equation with an input current which obeyed a first order partial differential equation. This model bears the same relation to the purely white-noise driven cable [14] as Stein's model with two components [15,16] does to the original one-component model [17]. The effect of the additional components is to make the time-courses of postsynaptic potentials smoother, more in accordance with observation. It is noteworthy, however, that in cable models, there is smoothing also if the observation point is remote from the point at which the synaptic input occurs. Relatively few articles have addressed analytically the properties of cable model neurons with noise, but an interesting investigation oriented towards the signal processing capabilities of neurons with various sources of fluctuation was carried out by Manwani and Koch [18,19].

2. Model description

Let $V(x, t)$ be the depolarization from resting potential at time t and space point x with corresponding input current density $I(x, t)$. Then, in the form explicitly showing the biophysical parameters of the neuron [20] we have for the stochastic partial differential equations describing the model,

$$r_m c_m \frac{\partial V}{\partial t} = -V + \frac{r_m}{r_i} \frac{\partial^2 V}{\partial x^2} + r_m I, \quad 0 < x < l, \quad t > 0, \quad (2.1)$$

where $I = I(x, t)$ is the input current density. We will distinguish between excitatory and inhibitory input streams by letting $\{N_E(x, t), 0 < x < l, t \geq 0\}$ and $\{N_I(x, t), 0 < x < l, t \geq 0\}$ be two-parameter stochastic counting processes for the numbers of excitatory and inhibitory synaptic inputs. That is, for example, $N_E(x, t)$ is a random variable representing the number of points in the

rectangle $(0, x] \times (0, t]$ at which excitatory inputs arrive. In general, the current density satisfies the partial differential equation

$$\frac{\partial I}{\partial t} = -\frac{I}{\tau_c} + a_E(x, t) \frac{\partial^2 N_E}{\partial x \partial t} - a_I(x, t) \frac{\partial^2 N_I}{\partial x \partial t}, \quad (2.2)$$

where τ_c is the time constant of decay of the current (which might in fact depend on x) and where $a_E, a_I \geq 0$ describe the excitatory and inhibitory event amplitudes as functions of space and time. The corresponding rate functions are defined as $\lambda_E(x, t)$ and $\lambda_I(x, t)$ with

$$E\left(\frac{\partial^2 N_E(x, t)}{\partial x \partial t}\right) = \lambda_E(x, t)$$

and

$$E\left(\frac{\partial^2 N_I(x, t)}{\partial x \partial t}\right) = \lambda_I(x, t),$$

where E denotes expectation.

The expected values of N_E and N_I are thus

$$E(N_{E,I}(x, t)) = \int_0^t \int_0^x \lambda_{E,I}(y, s) ds dy.$$

Note that if (x_0, t_0) is a space–time point at which an excitatory event occurs, then the contribution to $\frac{\partial I}{\partial t}$ is $a_E(x_0, t_0)\delta(x - x_0)\delta(t - t_0)$ and similarly for inhibition. In [Table 1](#) are given the units and meanings of the various symbols for the variables and parameters before and after the following change of variables.

2.1. Change of variables and the diffusion approximation

It is convenient to change variables in order to reduce the number of constants appearing in the equations. To this end, we put

$$X = \frac{x}{\lambda}, \quad T = \frac{t}{\tau_m}$$

so distances are in space constants and time in time constants. We also introduce $\bar{c}_m = \lambda c_m$ which is the capacitance of a characteristic length of membrane and put $\bar{V}(X, T) = V(x, t)$, $\bar{I}(X, T) = \lambda \tau_m I(x, t)$, $\bar{N}_{E,I}(X, T) = N_{E,I}(x, t)$, $\bar{a}_{E,I}(X, T) = \tau_m a_{E,I}(x, t)$ so that the differential equations become

$$\frac{\partial \bar{V}}{\partial T} = -\bar{V} + \frac{\partial^2 \bar{V}}{\partial X^2} + \frac{\bar{I}}{\bar{c}_m}, \quad 0 < X < L, \quad T > 0, \quad (2.3)$$

$$\frac{\partial \bar{I}}{\partial T} = -\alpha \bar{I} + \bar{a}_E(X, T) \frac{\partial^2 \bar{N}_E}{\partial X \partial T} - \bar{a}_I(X, T) \frac{\partial^2 \bar{N}_I}{\partial X \partial T}, \quad (2.4)$$

where we have put $\alpha = \frac{\tau_m}{\tau_c}$ and $L = \frac{l}{\lambda}$. We will also put

Table 1
Variables and biophysical parameters

Symbol	Description of quantity	Units
x	Distance along neuron	cm
t	Time since beginning of ‘experiment’	s
l	Length of neuron	cm
r_m	Membrane resistance of unit length times unit length	ohm cm
c_m	Membrane capacitance per unit length	Farads/cm
r_i	Internal resistance per unit length	Ohm/cm
λ	Membrane characteristic length, $\sqrt{\frac{r_m}{r_i}}$	cm
τ_m	Membrane time constant, $c_m r_m$	s
$V(x, t)$	Depolarization from resting potential	V
$I(x, t)$	Current density	A/cm
τ_c	Time constant of decay of current	s
$N_{E,I}(x, t)$	Count of number of excitatory (inhibitory) events	Dimensionless
$a_{E,I}(x, t)$	Amplitude of excitatory (inhibitory) events	A
$\lambda_{E,I}(x, t)$	Mean rate of arrival of excitation (inhibition)	per cm second
X, T	Dimensionless distance, x/λ and time, t/τ_m	Dimensionless
$\bar{V}(X, T)$	Depolarization at (X, T)	V
$\bar{I}(X, T)$	$\tau_m \lambda I(x, t)$	C
$\bar{N}_{E,I}(X, T)$	Count of number of excitatory (inhibitory) events	Dimensionless
$\bar{\lambda}_{E,I}(X, T)$	Mean rate of arrival of excitation (inhibition) $\lambda \tau_m \lambda_{E,I}$	Dimensionless
$\bar{a}_{E,I}(X, T)$	Amplitudes $\tau_m a_{E,I}(x, t)$	C
α	Ratio of membrane to current time-constant τ_m/τ_c	Dimensionless
ρ_{IE}	Ratio of inhibitory to excitatory input frequency (uniform)	Dimensionless
t_R	Refractory period in time constants	Dimensionless

$$\bar{\lambda}_{E,I}(X, T) = \lambda \tau_m \lambda_{E,I}(x, t).$$

We wish to consider a diffusion-type approximate version of (2.4) and thus introduce the drift

$$\mu(X, T) = \bar{a}_E(X, T) \bar{\lambda}_E(X, T) - \bar{a}_I(X, T) \bar{\lambda}_I(X, T)$$

and noise amplitude

$$\sigma(X, T) = \sqrt{\bar{a}_E^2(X, T) \bar{\lambda}_E(X, T) + \bar{a}_I^2(X, T) \bar{\lambda}_I(X, T)}.$$

A two-parameter white noise replaces the derivatives of the Poisson processes so that the differential equation for \bar{I} is now

$$\frac{\partial \bar{I}}{\partial T} = -\alpha \bar{I} + \mu(X, T) + \sigma(X, T) \frac{\partial^2 W}{\partial X \partial T}, \quad 0 < X < L, \quad T > 0, \tag{2.5}$$

where W is a standard two-parameter Wiener process or Brownian motion. Eqs. (2.3) and (2.5) describe the model we wish to consider in dimensionless space–time. We will use it to compute statistical properties of neurophysiological variables in the remainder of this article. Note that the synaptic reversal potentials first employed in stochastic modeling in [21] and conductance-based changes for synaptic action are lumped into the additive synaptic current terms; cf [6].

From the standard theory for linear partial differential equations, the voltage \bar{V} at each X and T is the random variable

$$\bar{V}(X, T) = \int_0^L G(X, Y; T) \bar{V}(Y, 0) dY + \frac{1}{\bar{c}_m} \int_0^L \int_0^T G(X, Y; T - S) \bar{I}(Y, S) dS dY, \quad (2.6)$$

where G is the Green's function for the cable equation $\bar{V}_T = -\bar{V} + \bar{V}_{XX}$ for given boundary conditions and $\bar{V}(Y, 0)$ is the initial potential, which at each Y may be a random variable. This relation was exploited in [13] to find analytical expressions for several statistical properties of the potential in subthreshold states, including moments and spectral density, for various boundary conditions. Most expressions obtained assumed that the amplitude and rate functions were constant throughout the length of the neuron.

3. Effects on spiking of spatial synaptic input patterns

We assume that the amplitude and rate functions only depend on position which is equivalent to assuming that the input Poisson processes are temporally homogeneous but not necessarily spatially homogeneous. However, changes in synaptic strength or rates in time can be easily implemented.

Assuming the potential is uniformly at rest at $T = 0$, from [13] the mean voltage is given by

$$E[\bar{V}(X, T)] = \frac{1}{\bar{c}_m} \int_0^L \int_0^T G(X, Y; T - S) e^{-\alpha S} \times \left[\int_0^S e^{\alpha U} \{ \bar{a}_E(Y) \bar{\lambda}_E(Y) - \bar{a}_I(Y) \bar{\lambda}_I(Y) \} dU \right] dS dY. \quad (3.1)$$

For cables of finite length, the Green's function can be written as a Fourier series

$$G(X, Y; T) = \sum_n \phi_n(X) \phi_n(Y) e^{-\lambda_n T}, \quad T > 0, \quad (3.2)$$

where $\{\phi_n\}$ is the set of normalized spatial eigenfunctions and $\{\lambda_n\}$ is the set of corresponding eigenvalues. In general, if we put

$$F(Y) = \bar{a}_E(Y) \bar{\lambda}_E(Y) - \bar{a}_I(Y) \bar{\lambda}_I(Y),$$

which describes the net synaptic drive in $(Y, Y + dY)$, then the mean depolarization is found to be

$$E[\bar{V}(X, T)] = \frac{1}{\alpha \bar{c}_m} \sum_n \phi_n(X) \Phi_n(L) \left\{ \frac{1 - e^{-\lambda_n T}}{\lambda_n} - \frac{(e^{-\alpha T} - e^{-\lambda_n T})}{\lambda_n - \alpha} \right\},$$

where we have defined

$$\Phi_n(L) = \int_0^L \phi_n(Y) F(Y) dY,$$

and it is assumed that $\lambda_n \neq \alpha$ for any n . In the event that $\lambda_n = \alpha$, the corresponding term in curly brackets is replaced by

$$\left\{ \frac{1 - e^{-\lambda_n t}}{\lambda_n} - t e^{-\lambda_n t} \right\}.$$

Several types of boundary condition may be employed for the cable equation (2.3) and for each type there is a different G . Even the rather complicated lumped-soma boundary condition [20, chapter 6] gives an incomplete picture because the axon is ignored. If the latter is included, the treatment will depend on the nature of the myelination. Since we are concerned with gaining some insight into the effects of various patterns of input, a reasonable choice of boundary condition is to employ sealed end conditions at both $X=0$ and $X=L$. In this case, the eigenvalues are

$$\lambda_n = 1 + n^2 \pi^2 / L^2, \quad n = 0, 1, \dots$$

and the normalized (to unity) eigenfunctions are

$$\phi_n(X) = \begin{cases} \frac{1}{\sqrt{L}}, & n = 0, \\ \sqrt{2/L} \cos(n\pi X/L), & n = 1, 2, \dots \end{cases}$$

Standard parameter values. We use parameter values which are based on those appropriate for pyramidal cells. However, because information is patchy we have to also draw on values for other cells such as spinal motoneurons. The value of τ_c is obtained from [22]. The membrane time-constant τ_m was set at 30 ms after reference [23]. Using these two time-constants gives $\alpha = 10$, but a much smaller value would be appropriate for motoneurons. The threshold condition is an approximation only and the voltage criterion used was $\theta = 10$ mV, which is in the lower end of the range. Larger values would of course lead to longer interspike intervals with an approximately exponential relationship. The space-constant λ was estimated by scaling from the motoneuron value of R_m to that of a pyramidal cell which is 16 times greater [23] and using r_i appropriate for a cylinder of diameter 10 μm . The electrotonic length of the nerve cylinder was set at 2, corresponding to a physical length of 7.6 mm, which is reasonable for large pyramidal cells in layer 5.

The rates of background excitatory and inhibitory synaptic input are obtained from the data of [24,25] assuming 8250 excitatory synapses with average frequencies of 1 Hz and 1475 inhibitory synapses with average frequencies of 5.5 Hz. These data give 165000 excitatory events per cm per second which for the assumed cylinder of $L=2$ and diameter 10 μm translates to $\bar{\lambda}_E = 1881$ (dimensionless) and $\bar{\lambda}_I = 0.98\bar{\lambda}_E$. To estimate a_E a charge of 3×10^{-10} C was assumed to be delivered during a 5 ms period to give a current of 0.6×10^{-7} A. This gives $\bar{a}_E = 0.03 \times 0.6 \times 10^{-7}$. The magnitude of \bar{a}_I was set equal to that of \bar{a}_E . The standard parameter values used are summarized in Table 2.

3.1. Uniform stimulation

When sealed end conditions are employed and the synaptic drive does not depend on position so that

$$F(Y) = \bar{a}_E \bar{\lambda}_E - \bar{a}_I \bar{\lambda}_I$$

the mean voltage is found to be independent of X ,

Table 2
Standard parameter set

Parameter	Value
τ_c	3 ms
τ_m	30 ms
α	10 (dimensionless)
θ	10 mV
λ	3.8 mm
L	2 (dimensionless)
$\bar{\lambda}_E$	1881 (dimensionless)
$\bar{\lambda}_I$	$0.983\bar{\lambda}_E$ (dimensionless)
\bar{a}_E	$0.03 \times 0.6 \times 10^{-7}$ (dimensionless)
\bar{a}_I	$0.03 \times 0.6 \times 10^{-7}$ (dimensionless)

$$E[\bar{V}(X, T)] = \frac{\bar{a}_E \bar{\lambda}_E - \bar{a}_I \bar{\lambda}_I}{\alpha \bar{c}_m} \left[1 - e^{-t} + \frac{1}{1 - \alpha} (e^{-t} - e^{-\alpha t}) \right], \quad \alpha \neq 1.$$

When $\alpha = 1$, this is

$$E[\bar{V}(X, T)] = \frac{\bar{a}_E \bar{\lambda}_E - \bar{a}_I \bar{\lambda}_I}{\bar{c}_m} [1 - e^{-t}(t + 1)].$$

3.1.1. Approximate firing rates

Assume that a threshold voltage θ must be reached at some point along the neuron for an action potential to be emitted. Then an estimate \hat{T}_θ may be made of the time T_θ at which $\bar{V}(X, T)$ reaches threshold, assuming

- (a) the steady state value $(\bar{a}_E \bar{\lambda}_E - \bar{a}_I \bar{\lambda}_I) / (\alpha \bar{c}_m) \gg \theta$
- (b) the standard deviation of $\bar{V}(X, T)$ (see Section 3.2.1 of Ref. [13]) is small relative to $E[\bar{V}(X, T)]$ for $t < E[T_\theta]$.

The validity of (a) is not dependent on X but this is not the case for condition (b). If we consider just the point $X = 0$, using the steady state value standard deviation [13] and of the mean, the condition (b) becomes approximately

$$\sigma \left[\frac{1}{1 + \alpha} + \sum_{n=1}^{\infty} \frac{2}{(1 + \lambda_n^2)(1 + \alpha + \lambda_n^2)} \right]^{\frac{1}{2}} \leq K \sqrt{\frac{2L}{\alpha \bar{c}_m}},$$

where $K = \bar{a}_E \bar{\lambda}_E - \bar{a}_I \bar{\lambda}_I$ and $\sigma = \sqrt{\bar{a}_E^2 \bar{\lambda}_E + \bar{a}_I^2 \bar{\lambda}_I}$. The estimated mean ISI is made from the implicit relation

$$E[\bar{V}(X, \hat{T}_\theta)] = \theta, \tag{3.3}$$

and the calculated firing rate is then determined from

$$f = \frac{1}{E[\hat{T}_0] + t_R},$$

where t_R is a refractory period.

In Fig. 1, we show the firing frequency of the given model neuron calculated by using (3.3). Here we have used the standard parameters but let the ratio of the frequency of inhibition to that of excitation,

$$\rho_{IE} = \frac{\bar{\lambda}_I}{\bar{\lambda}_E},$$

vary from the standard value of 0.98 to nearly unity. The expected time to reach threshold when $\rho = 0.98$ is 0.0969 time constants which gives a very high firing rate of 169 Hz assuming $t_R = 0.1\tau_m$. Small increases in ρ lead to very large changes in the output frequency. Thus when $\rho = 0.995$ the mean time for V to reach threshold has more than doubled at $E[\hat{T}_0] = 0.2382\tau_m$ with a firing rate of 98.6 Hz; and when ρ_{IE} is only slightly further increased to $\rho_{IE} = 0.9993$, the value of $E[\hat{T}_0] = 3.276\tau_m$ and the frequency of firing is only 9.6 Hz.

Balanced inputs. The term ‘balanced’ has been employed to describe the rough equality of excitatory and inhibitory inputs to cortical neurons [26,27] and the standard parameter values that we have employed are close to those of the balanced input paradigm. It is remarkable that small changes from the (approximately) balanced condition lead to such radical changes in output firing frequency. This means that if the ‘normal’ or ‘usual’ values of the input rates and amplitudes, taking also into account their spatial distributions over the postsynaptic neuron’s surface, are near a

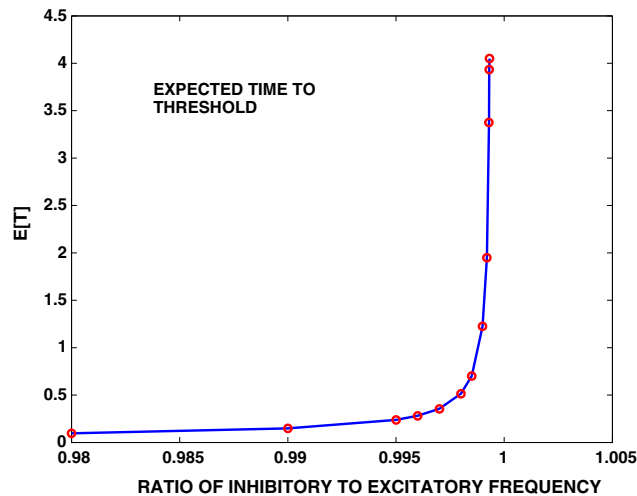


Fig. 1. The blue curve shows the approximate expected time, in time constants, for the depolarization to reach threshold as the fraction of inhibitory input frequency grows relative to the excitatory input frequency. The black curve shows the mean firing frequency in Hertz assuming a refractory period of 3 ms and a time constant of 30 ms. Parameters are appropriate for pyramidal cells. Points (red circles and blue diamonds) obtained from solutions of (3.3). (For interpretation of the references to colour in this figure legend the reader is referred to the web version of this article.)

balanced state then a small shift in any one of the quantities (a) frequency of excitation, (b) frequency of inhibition, (c) amplitude of excitation, (d) amplitude of inhibition, will lead to either a state of much larger output frequency or a state of much decreased output frequency. From a network point of view, if many connected cells undergo similar input parameter changes, then the network may become over-excited and over-synchronized or, on the other hand, it may become effectively silent. These conclusions would also be obtained from other models, including conductance-based non-linear models of Hodgkin–Huxley type or even one-dimensional integrate-and-fire models. The existence of small shifts in excitatory postsynaptic current amplitudes due to the presence of a genetic mutation in Rett's syndrome has recently been confirmed experimentally [28]. Such small changes lead to very large changes in the activity of the neurons affected.

3.1.2. Simulation method and results

In [13], it was shown that for finite-length cables, the potential $V(X, \cdot)$ at any space point could be represented in terms of one-dimensional random processes as follows. Recall that $\bar{V}(X, T)$ can be written as

$$\bar{V}(X, T) = E[\bar{V}(X, T)] + \bar{V}_R(X, T)$$

where \bar{V}_R is a purely random component while $E[\bar{V}(X, T)]$ is purely deterministic. In the case of constant σ and a bounded space interval it was shown that if we define the processes

$$W_n(t) = \int_a^b \int_0^t \phi_n(y) dW(y, s), \quad t \geq 0,$$

$$U_n(s) = e^{-\alpha s} \int_0^s e^{\alpha u} dW_n(u), \quad s \geq 0$$

and

$$V_n(t) = \int_0^t e^{-\lambda_n(t-s)} U_n(s) ds$$

then the following explicit series representation holds

$$\bar{V}_R(X, T) = \sigma \sum_n \phi_n(X) V_n(T)$$

in which individual terms are independent. Furthermore, the following system of stochastic differential equations holds

$$d \begin{bmatrix} U_n \\ V_n \end{bmatrix} = \begin{bmatrix} -\alpha & 0 \\ 1 & -\lambda_n \end{bmatrix} \begin{bmatrix} U_n \\ V_n \end{bmatrix} dt + \begin{bmatrix} dW_n \\ 0 \end{bmatrix}.$$

To simulate a path for $\bar{V}(x, t)$ at fixed x , we may therefore use the following Euler-type iterative formulas in conjunction with the expected value of $\bar{V}(x, t)$

$$U_n(t + \Delta t) = U_n(t) - \alpha U_n(t) \Delta t + N(0, 1) \sqrt{\Delta t}$$

$$V_n(t + \Delta t) = V_n(t) - \lambda_n V_n(t) \Delta t + U_n(t) \Delta t$$

$$\bar{V}_R(x, t + \Delta t) = \bar{V}_R(x, t) + \sigma \Delta t \sum_n \phi_n(x) [U_n(t) - \lambda_n V_n(t)].$$

Here $N(0, 1)$ is a member of a sequence of independent standard normal random variables.

The method of simulation was applied to determine model neuronal response with the standard parameter set as indicated in Table 2. It became apparent after a few trials that due to the large variability in the input processes with these parameters and due to the fact that the chances of inhibition and excitation were almost equal, the voltage trajectories would sometimes spend very large amounts of time at very hyperpolarized states. In real neurons such excursions are prevented by the inhibitory reversal potential. In order to prevent such excursions, it was decided to put a reflecting barrier at -10 mV, which is roughly the value of the inhibitory reversal potential. The resulting interspike intervals were almost the same as those obtained without the reflecting barrier, which indicates that if a sequence of inputs is inhibition dominated then it matters not much if the voltage is allowed to wander around at large negative values because if the inhibitory reversal potential was included the voltage would spend an almost equivalent long time at that reversal potential. The similarity of the results with and without the reflecting barrier are illustrated in Fig. 2, where histograms of the ISI are shown in the two cases for 1000 trials each. With the reflective barrier at -10 mV (left histogram), the mean ISI was 0.1509, the standard deviation was 0.2724 and the coefficient of variation (CV), 1.81. Without the barrier these three quantities were 0.1773, 0.3319 and 1.87, respectively. In most other cases examined, the difference between the

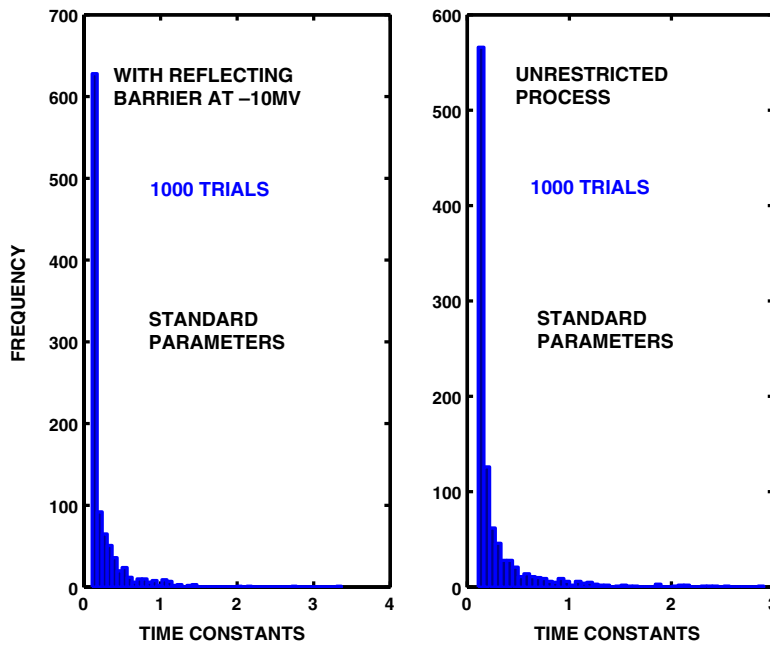


Fig. 2. ISI histograms from simulation for the case of uniform stimulation and the standard parameter set. On the left is the result when a reflecting barrier is placed at -10 mV relative to resting level, whereas on the right is shown the histogram of interspike intervals obtained for the unrestricted membrane potential process.

Table 3

Mean ISI results for uniform stimulation with the standard parameter set, as ρ_{IE} , the ratio of inhibition to excitation varies

ρ_{IE}	Mean Eq. (3.3)	Mean $\sigma = 0.05$	Mean ISI	Standard deviation	Coefficient of variation
0.98	0.097	0.113	0.186	0.326	1.76
0.99	0.148	0.162	0.206	0.411	1.99
0.995	0.238	0.255	0.263	0.540	2.05
0.999	1.224	1.245	0.287	0.618	2.16

two sets of results was very small so that for the rest of the reported results in this article, no barrier was in place.

Simulations were performed with the standard parameter set for several values of ρ_{IE} near the value 1. The results are summarized in Table 3. In column 2 are shown the results from (3.3) (no noise), these points having also being plotted in Fig. 1. Column 3 shows the mean ISI for the same mean input but with the deliberately chosen small value of σ of 0.05. It can be seen that good agreement is obtained between the simulation results with small noise and the analytical approach employing (3.3). In columns 4, 5 and 6 are the mean, standard deviation and CV from simulation (500 trials) with σ given by the actual value

$$\sigma = \sqrt{\bar{a}_E^2 \bar{\lambda}_E + \bar{a}_I^2 \bar{\lambda}_I}.$$

The mean ISIs in columns 2 and 3 (noise-free, (3.3) and small σ simulation) are always in good agreement. However, the full noise mean ISI (column 4) departs further from the columns 2 and 3 results as ρ_{IE} increases, even though the increases are not large. As more inhibition is included, the mean ISI increases as expected, but not to the same extent as in the noise-free or small σ cases. Evidently, the large fluctuations obtained when the full noise is included make fast transitions to threshold much more likely. As ρ_{IE} increases, the mean, standard deviation and CV of the ISI increase, the CV eventually attaining quite large values of over 2.

3.2. Effects of non-uniform stimulation

It is well known that distributions of excitation and inhibition are not uniform over the somadendritic surfaces of most neurons, including cortical and other pyramidal cells. For the latter, there is a preponderance of inhibition nearer the soma [24,26,29]. We will attempt to explore briefly a uniform versus non-uniform distribution of synaptic input as follows. We restrict our attention here to cases where the noise amplitude function is constant, despite the variations in synaptic strengths.

Uniform case. We let both excitation and inhibition be uniformly distributed over the neuronal surface. The function $\bar{a}_E(X)$ is set at the usual value \bar{a}_E for all $X \in (0, L)$ and the function $\bar{a}_I(X)$ is set at $-\bar{a}_E$. The function $\bar{\lambda}_E(X) = \bar{\lambda}_E$ for all $X \in (0, L)$ and the function $\bar{\lambda}_I(x) = \bar{\lambda}_E$ for all $X \in (0, L)$. With these values we find for all $X \in (0, L)$

$$\mu(X) = 0,$$

$$\sigma(X) = \bar{a}_E \sqrt{2\bar{\lambda}_E}.$$

Simulation, based on 1000 trials, was used to estimate the ISI for this case uniform stimulation using standard values for \bar{a}_E and $\bar{\lambda}_E$. This gave values of the mean, standard deviation and CV of the ISI as 0.2784, 0.5767 and 2.07, respectively. The histogram of ISI values was similar in shape to those of Fig. 2.

Non-uniform case. For a simple example of non-uniform synaptic input, we have placed the same *total* excitation and inhibition as in the uniform case but now the inhibition is uniformly distributed on the proximal part (0, $L/2$) and the excitation is uniformly distributed on the distal

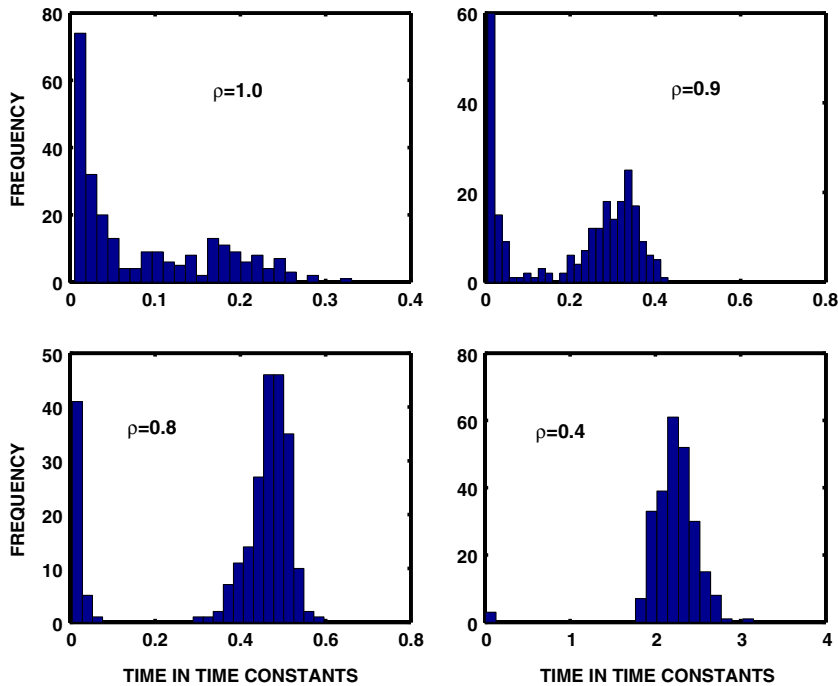


Fig. 3. Interspike interval histograms for various values of the parameter ρ which determines the background level of excitation. For $\rho = 1$ there is no inhibition but excitation in the distal half of the cell. As ρ decreases, more inhibition appears in the proximal part of the neuron’s dendritic tree so that eventually when $\rho = 0$ there are equal amounts of inhibition and excitation with proximal inhibition and distal excitation.

Table 4
Mean ISI results for non-uniform stimulation as described above as the additive current parameter ρ varies

ρ	Mean ISI	St. Dev.	CV
1.0	0.087	0.081	0.926
0.9	0.203	0.142	0.699
0.8	0.385	0.181	0.471
0.7	0.595	0.177	0.298
0.6	0.849	0.194	0.229
0.5	1.240	0.248	0.200
0.4	2.220	0.325	0.146

part $(L/2, L)$. Thus $\bar{a}_I(X) = -\bar{a}_E$ and $\bar{\lambda}_I(X) = 2\bar{\lambda}_E$ for $0 < X < L/2$, zero otherwise, and $\bar{a}_E(X) = \bar{a}_E$ and $\bar{\lambda}_E(X) = 2\bar{\lambda}_E$ for $L/2 < X < L$ and zero otherwise. We also insert an adjustable uniform constant background input of $2\rho\bar{\lambda}_E\bar{a}_E$, where $0 \leq \rho \leq 1$. This gives

$$\mu(X) = \begin{cases} 2\bar{\lambda}_E\bar{a}_E[\rho - 1], & 0 < X < L/2, \\ 2\bar{\lambda}_E\bar{a}_E[\rho + 1], & L/2 < X < L, \end{cases}$$

and $\sigma(X) = 2\bar{a}_E\sqrt{\bar{\lambda}_E}$ is the same. Note that the stimulation is non-uniform for all ρ . When $\rho = 1$ there is zero input for $(0, L/2)$ and excitation on $(L/2, L)$, and when $\rho = 0$ there is inhibition on $(0, L/2)$ and excitation of the same strength on $(L/2, L)$. The same standard amplitude (\bar{a}_E) was employed in simulations for this case. The threshold point for action potential generation is, as throughout, $X = 0$.

Simulations were performed for various values of ρ with 500 trials and a time-step of 0.0002 s or less. The histograms for the ISI for several values of ρ are shown in Fig. 3. For $\rho = 1$, when there is in fact no inhibition, the histogram is similar to those of Fig. 2. When the amount of inhibition towards the soma ($X = 0$) is increased slightly ($\rho = 0.9$), the density of the ISI starts to increase at large times and decrease at small times, giving the distribution a bimodal form. As the amount of inhibition near the soma increases, and concomitantly the amount of excitation in the distal parts of the cell decreases, the peak near the origin drops and the one at large times grows. Eventually, at $\rho = 0.4$ the ISI distribution is again almost unimodal, but the mass is isolated from the origin as small intervals are absent. It achieves a Gaussian-type appearance with its mean and mass at a large distance from the origin. This is one of the few examples (that is for $\rho = 0.9$ – 0.5) where a bimodal distribution is encountered for the ISI in a neural model where the subthreshold behaviour is linear, although the phenomenon would probably occur in the standard cable model [14], although bimodality has been observed in more complex models of cortical pyramidal cells [31].

The corresponding results for the mean, standard deviation and CV of the ISI for various values of ρ are given in Table 4. As ρ decreases, the mean ISI increases quite sharply, but the standard deviation increases much more slowly, resulting in a rapidly declining CV, which by $\rho = 0.4$ is only 16% of its value when $\rho = 1$.

4. Discussion

Experimental observations on the trains of spikes emitted by neurons almost anywhere in the mammalian central nervous system reveal that they are usually essentially stochastic. The meaning or relevance of such apparent randomness is not clear [11]. Models to study such phenomena may be solved using numerical or analytical methods, or a combination as in the present paper. In the last 50 years, a gamut of mathematical stochastic models has been proposed, beginning with simple perfect integrator models employing unfiltered Brownian motion and one-dimensional leaky-integrate-and-fire (LIF) models which often entail an Ornstein–Uhlenbeck process whose study has been very fruitful.

We have chosen a model which increases the amount of physiological reality over simple cable models by including current decay on arrival of postsynaptic potentials. Including a

space-dimension is valuable for considering the effects of different spatial distributions of the various synaptic inputs which bombard a cortical cell's surface, usually at an extremely high rate. In the present model, the differential equation for the synaptic current is driven by an two-parameter Poisson processes, so that the neuron is represented by a system of two coupled stochastic partial differential equations rather than one. We turned to a diffusion approximation in which the Poisson noise was replaced by Gaussian 2-parameter white noise. This gave a current which we call a two-parameter Ornstein–Uhlenbeck process. In an earlier publication [13], we obtained expressions for most of the usually studied statistical properties of the voltage in the absence of a threshold for firing.

A standard set of parameters was extracted from the available literature on cortical pyramidal cells, but the accuracy of these data is not guaranteed as they come from disparate sources. The values employed for the input parameters $\bar{\lambda}_{E,I}$ and $\bar{a}_{E,I}$ give rise to a near balanced condition, which means the drift is often small but the noise is large. We were able to relate the results on firing rates around the balance point to the synaptic input situation in Rett's syndrome (smaller values of \bar{a}_E).

The changes in the probability distribution and the CV of the ISI as the spatial distribution of inhibition and excitation change are the most interesting aspects of the results we have obtained. However, it remains an important project for future work to study more closely the effects that various spatial distributions have, as previous studies of balanced inputs have usually been made with one-dimensional models [27,30] with which an accurate study of spatial distributions is not possible.

Acknowledgements

The author thanks the Max Planck Institute for financial support and Prof. Dr. Juergen Jost for his kind hospitality. I am also grateful to Prof. Dr. Luigi M. Ricciardi for the invitation to present this work at Biocomp 2005.

References

- [1] M.N. Shadlen, W.T. Newsome, The variable discharge of cortical neurons: implications for connectivity, computation and information coding, *J. Neurosci.* 18 (1998) 3870.
- [2] W.R. Softky, C. Koch, The highly irregular firing of cortical cells as inconsistent with temporal integration of random EPSPs, *J. Neurosci.* 13 (1993) 334.
- [3] G.L. Gerstein, N.Y.-S. Kiang, An approach to the quantitative analysis of electrophysiological data from single neurons, *Biophys. J.* 1 (1960) 15.
- [4] E.V. Evarts, Temporal patterns of discharge of pyramidal tract neurons during sleep and waking in the monkey, *J. Neurophysiol.* 27 (1964) 152.
- [5] B.D. Burns, A.C. Webb, The spontaneous activity of neurones in the cat's cerebral cortex, *Proc. Soc. Lond. B* 194 (1976) 211.
- [6] P.H.E. Tiesinga, J.V. Jose, T.J. Sejnowski, Comparison of current-driven and conductance-driven neocortical model neurons with Hodgkin–Huxley voltage-gated channels, *Phys. Rev. E* 62 (2000) 8413.
- [7] A. Destexhe, M. Rudolph, Extracting information from the power spectrum of synaptic noise, *J. Comp. Neurosci.* 17 (2004) 327.

- [8] H. Meffin, A.N. Burkitt, D.B. Grayden, An analytical model for the “large, fluctuating conductance state” typical of neocortical neurons *in vivo*, *J. Comp. Neurosci.* 16 (2004) 159.
- [9] K. Diba, H.A. Lester, C. Koch, Intrinsic noise in cultured hippocampal neurons: experiment and modeling, *J. Neurosci.* 24 (2004) 9723.
- [10] H.C. Tuckwell, Spike trains in a stochastic Hodgkin–Huxley system, *BioSystems* 80 (2005) 25.
- [11] R.B. Stein, E.R. Gossen, K.E. Jones, Neuronal variability: noise or part of the signal? *Nat. Rev. Neurosci.* 6 (2005) 389.
- [12] J. Fiser, C. Chiu, M. Weliky, Small modulation of ongoing cortical dynamics by sensory input during natural vision, *Nature* 431 (2004) 573.
- [13] H.C. Tuckwell, Spatial neuron model with two-parameter Ornstein–Uhlenbeck input current, *Physica A* 368 (2006) 495.
- [14] H.C. Tuckwell, J.B. Walsh, Random currents through nerve membranes, *Biol. Cybernet.* 49 (1983) 99.
- [15] H.C. Tuckwell, F.Y.M. Wan, J.-P. Rospars, A spatial stochastic neuronal model with Ornstein–Uhlenbeck input current, *Biol. Cybernet.* 86 (2002) 137.
- [16] N. Brunel, S. Sergi, Firing frequency of leaky integrate-and-fire neurons with synaptic current dynamics, *J. Theor. Biol.* 195 (1998) 87.
- [17] R.B. Stein, A theoretical analysis of neuronal variability, *Biophys. J.* 5 (1965) 173.
- [18] A. Manwani, C. Koch, Detecting and estimating signals in noisy cable structures, I: neuronal noise sources, *Neural Comput.* 11 (1999) 1797.
- [19] A. Manwani, C. Koch, Detecting and estimating signals in noisy cable structures, II: information theoretical analysis, *Neural Computat.* 11 (1999) 1831.
- [20] Tuckwell, H.C. Introduction to Theoretical Neurobiology, vol. 1, Linear cable theory and dendritic structure. Cambridge University, Cambridge, 1988.
- [21] H.C. Tuckwell, Synaptic transmission in a model for stochastic neural activity, *J. Theor. Biol.* 77 (1979) 65.
- [22] A. Destexhe, Z. Mainen, T.J. Sejnowski, Synthesis of models for excitable membranes, synaptic transmission and neuromodulation using a common kinetic formalism, *J. Comp. Neurosci.* 1 (1994) 195.
- [23] Z.F. Mainen, J. Joerges, J.R. Huguenard, T.J. Sejnowski, A model of spike initiation in neocortical pyramidal neurons, *Neuron* 15 (1995) 1427.
- [24] A. Destexhe, D. Paré, Impact of network activity on the integrative properties of neocortical pyramidal neurons *in vivo*, *J. Neurophysiol.* 81 (1999) 1531.
- [25] N. Iannella, H.C. Tuckwell, S. Tanaka, Firing properties of a stochastic PDE model of a rat sensory cortex layer 2/3 pyramidal cell, *Math. Biosci.* 188 (2004) 117.
- [26] M.N. Shadlen, W.T. Newsome, Noise, neural codes and cortical organization, *Curr. Opin. Neurobiol.* 4 (1994) 569.
- [27] A.N. Burkitt, Interspike interval variability for balanced networks with reversal potentials for large numbers of inputs, *Neurocomputing* 32–33 (2000) 313.
- [28] V. Dani et al., Reduced cortical activity due to a shift in the balance between excitation and inhibition in a mouse model of Rett’s syndrome, *PNAS (USA)* 102 (2005) 12560.
- [29] M. Megias et al., Total number and distribution of inhibitory and excitatory synapses on hippocampal cat pyramidal cells, *Neuroscience* 102 (2001) 527.
- [30] J. Feng, G. Wei, Increasing inhibitory input increases neuronal firing rate: why and when? Diffusion process case, *J. Phys. A* 34 (2001) 7493.
- [31] X.-J. Wang, Calcium coding and adaptive temporal computation in cortical pyramidal neurons, *J. Neurophysiol.* 79 (1998) 1549.